promoting access to White Rose research papers

Universities of Leeds, Sheffield and York
http://eprints.whiterose.ac.uk/

This is a copy of the final published version of a paper published via gold open access in **Engineering Structures**.

This open access article is distributed under the terms of the Creative Commons Attribution Licence (http://creativecommons.org/licenses/by/4.0/) which permits unrestricted use, distribution, and reproduction in any medium, provided the original work is properly cited.

White Rose Research Online URL for this paper:
http://eprints.whiterose.ac.uk/85981

Published paper

Londono, J.M., Neild, S.A. and Wagg, D.J. (2014) *Using a damper amplification factor to increase energy dissipation in structures*. Engineering Structures, 84. 162 - 171. Doi: 10.1016/j.engstruct.2014.11.019

White Rose Research Online
eprints@whiterose.ac.uk

Engineering Structures 84 (2015) 162–171

Contents lists available at ScienceDirect

Engineering Structures

journal homepage: www.elsevier.com/locate/engstruct

Using a damper amplification factor to increase energy dissipation in structures

Julián M. Londoño [a,*], Simon A. Neild [a], David J. Wagg [a,b]

[a] Department of Mechanical Engineering, University of Bristol, Queens Building, University Walk, Bristol BS8 1TR, UK
[b] Department of Mechanical Engineering, University of Sheffield, Sir Frederick Mappin Building, Mappin Street, Sheffield S1 3JD, UK

ARTICLE INFO

Article history:
Received 1 April 2014
Revised 2 September 2014
Accepted 17 November 2014
Available online 8 December 2014

Keywords:
Damping amplification
Energy dissipation
Real-time dynamic substructuring test
Structural control

ABSTRACT

Fluid dampers are an important tool for dissipating unwanted vibrations in a range of engineering structures. This paper examines the effects of amplifying the displacements transferred to a non-linear damper, to increase the effectiveness of the damper in a range of situations commonly encountered in civil engineering structures. These include, (i) the ability to "fine tune" the required damping for a particular size damper, (ii) the ability to have a set of the same size dampers, but with different amplification factors to achieve a specific damping task, and (iii) to increase the sensitivity of the damper to small movements which effectively extends the range over which the damper works. Through numerical simulations and experimental tests conducted on a non-linear damper, we quantify the potential advantages of adding an amplification factor and the range of parameters where the benefit to this device is significant. The example of a two-storey structure is used as a test case and real-time dynamic substructuring tests are used to assess the complete system performance using a range of different amplification factors. The results show that the structural performance is most improved for frequencies close to resonance and that the amplification factor has an effective limit that for the case considered in this study is of approximately 3. The effects of the mechanism compliance are also assessed.
© 2014 The Authors. Published by Elsevier Ltd. This is an open access article under the CC BY license (http://creativecommons.org/licenses/by/3.0/).

1. Introduction

The elimination of unwanted vibrations from civil engineering structures has been of growing importance in recent years, particularly for slender or otherwise flexible structures. This is important, not only for reducing the dynamic response of structures under extreme loads, but also for increasing the system reliability and ensuring human comfort during everyday dynamic loads [1]. Over recent decades improvement in damper technology have been seen. It is typical to split such technologies into three classes; (i) passive, (ii) active and (iii) semi-active devices [2]. In this paper, the focus is on using passive fluid dampers, in combination with a motion amplification mechanism. The purpose of the amplification factor is to increase the sensitivity of the damper and therefore extend its range of operation [3]. It can also be used to "tune" the required damping value of a single or multiple dampers.

In practice, the amplification factor can be achieved by using a variety of in-built mechanisms. In [3] for instance, dampers are connected to the structure through lever arms and double chevron braces. By selecting suitable lever arm ratios, the authors highlight that a single size of damper can be used throughout a building while still achieving the optimal response performance associated with using a range of damper sizes. However, the use of a chevron brace can be visually intrusive. A similar lever arm and chevron brace setup, this time utilising two dampers, is reported in [4], where the effects of brace stiffness is discussed. In [5] a brace system in which tensioned cables impose amplified structural displacements on dampers is presented. It is reported that this system can efficiently enhance damping without modifying the structural stiffness. However due to geometric limitations, the scheme is only able to deliver relatively low amplification. In [6] pre-tensioned diagonal bracing bars are connected to angular lever arms located at the lower corners of each bay. While offering a relatively unobtrusive solution, the performance is shown to be highly dependent on both the brace stiffness and its angle of inclination.

A toggle-brace-damper was proposed by Taylor Devices inc. in [7] and analysed in [8]. Despite being particularly sensitive to the brace stiffness, toggles can offer relatively high amplification factors. However, due to geometry considerations, the authors suggest a practical amplitude range of between 2 and 5. The use of MR dampers in conjunction with the toggle configuration is

* Corresponding author.
E-mail addresses: Julian.Londono@bristol.ac.uk (J.M. Londoño), Simon.Neild@bristol.ac.uk (S.A. Neild), David.Wagg@bristol.ac.uk (D.J. Wagg).

http://dx.doi.org/10.1016/j.engstruct.2014.11.019
0141-0296/© 2014 The Authors. Published by Elsevier Ltd.
This is an open access article under the CC BY license (http://creativecommons.org/licenses/by/3.0/).

discussed in [9]. They observed that the toggle configuration is likely to raise the structural stiffness. Scissor-jack-damper systems offer a compact method for high amplification, see for example the detailed assessment in [10]. However they also add stiffness and are sensitive to both pivot movement and elastic deformation. Another approach involves the use of gears. For example, a device constructed by coupling together two rack and two pinions having differing radii is described in [11]. The authors claim compactness and high amplification capability for the system. A further attractive approach, Hwang et al. [12], combines rotational inertia dampers with toggle bracing. In this case the amplification system is not only compact but also able to decrease the effective mass and stiffness of the structure.

Note that all of the mechanisms reported above have been modelled in the literature as constant amplification factors, i.e., coefficients that linearly scale the velocity transferred from the structure to the damper.

Here we are interested in the use of an amplifier in conjunction with a nonlinear damper for vibration suppression. Rather than studying a particular amplification mechanism, we wish to analyse how the combined nonlinearity and amplification changes the effectiveness of the vibration suppression. A further question is whether this behaviour results in an amplification limit beyond which no significant performance gain is obtained. Knowledge of this limit is needed to ensure well-behaved and cost-effective amplification mechanisms. As such we consider a generic amplifier capable of linearly scaling the displacement.

By considering a wide range of amplification factors and several loading conditions, we show both numerically and experimentally the advantages of amplifying the structural velocity transmitted to a small-scale non-linear damper. Using this approach we can identify the range of parameters where the most benefit is achieved when an amplification mechanism is added to the structure. We use the example of a two-storey structure to assess a whole system performance by considering a small non-linear damper attached to an amplification mechanism within the structure. A particular issue we consider is that of using an amplification mechanism-damper system with a smaller damper, to reduce the amount of stiction caused by large damper seals. The effects of the mechanism compliance are also assessed.

This paper is organised as follows. Section 2 introduces the structural model and highlights the effects of amplifying the velocity transferred to the non-linear dampers via numerical simulations. Section 3 presents details of the real-time dynamic substructuring, the experimental testing technique that has been used in this work. The numerical findings are validated experimentally through a series of experiments that physically test a real non-linear damper in Section 4. Finally, the conclusions and further remarks of this work are presented in Section 5.

2. Energy dissipation in dampers and the amplification factor

A basic approach for reducing structural vibration in buildings is to fit some supplemental damping devices into the structure. This concept takes advantage of the structure's own motion to produce relative movement within the damping devices. In response, those devices are expected to develop considerable local damping forces that act to dissipate a significant amount of energy—see for example [13] and references therein. If the relative motion of the damper can be amplified, then for small structural movements, a larger damping force can be achieved. Or, the same damping force can be achieved, but using a smaller damper.

Typical fluid dampers have a piston/plunger within a cylinder and two sets of seals. The seals are designed to maintain alignment of the damper and stop the fluid from leaking. In terms of damper performance the seals act as sources of non-linearity and friction effects. One consequence of the seals is that static friction will restrict the range of velocities when the damper will move. This results in two different types of behaviour (i) sticking when the force is below the static friction level and (ii) a slipping phase, after the damper is mobilised, where energy is effectively dissipated. It should be noted that negligible energy is dissipated in the damper during sticking and if there is a large range where this behaviour occurs the damper performance is degraded.

The major seismic building codes impose strict limits on the maximum permissible inter-storey drift of buildings when subject to earthquake excitation. While structural safety is the primary driver for these limits, minimising damage to non structural elements is also a factor when considering moderate or minor earthquakes. In fact, during moderate seismic events, structures are expected to exhibit just small lateral displacements. If the damper has been designed for a large event, small deformation may not even mobilise the damper, due to the internal friction forces that must be overcome prior to mobilisation of the damper.

Since energy is dissipated during the slipping phase rather than a sticking phase, one advantage of amplifying the structure's motion is to use a smaller dampers with lower static friction so that the slipping phase occurs at lower displacements (and velocities). The concept is illustrated in Fig. 1, which shows experimental results from a large-scale non-linear viscous fluid damper (NLD). Two experimental tests, one over a low and the other a high displacement range are shown. It can be seen that no slip occurs over the low range and hence the NLD effectively acts as a nonlinear spring rather than as an energy dissipator. The NLD has a peak force of 60 kN and a maximum stroke of ±15 mm [14]. When acting at a range of low displacements, the damper behaves as a very stiff spring, meanwhile at large displacements the damper goes into the slipping phase, describing the well-known hysteretic loop and dissipating energy. Therefore, in this situation, using smaller dampers and amplifying the structural motion transferred to them could significantly increase the dampers efficacy.

2.1. Two-storey example

As an example structure we consider a symmetric two-storey building with two NLD attached at the first floor as shown in Fig. 2a. The structure and damper size were tuned to produce an equivalent additional damping of approximately 20% of the critical damping ratio when the system oscillating at the frequency of the first linear mode. We note that this damper configuration may not

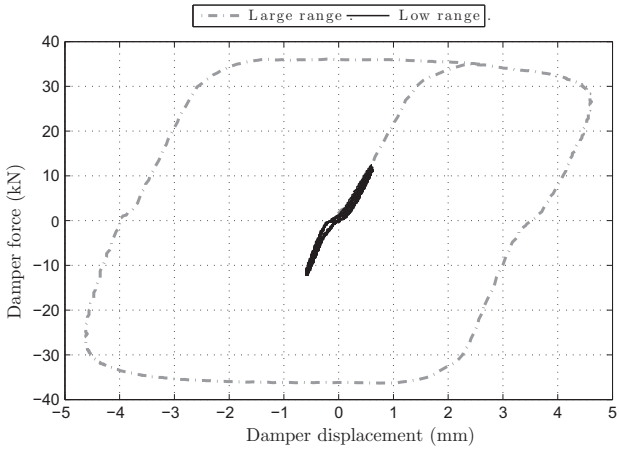

Fig. 1. Experimental data from a non-linear viscous fluid damper at low level (solid line) and large (dashed line) regime of displacements.

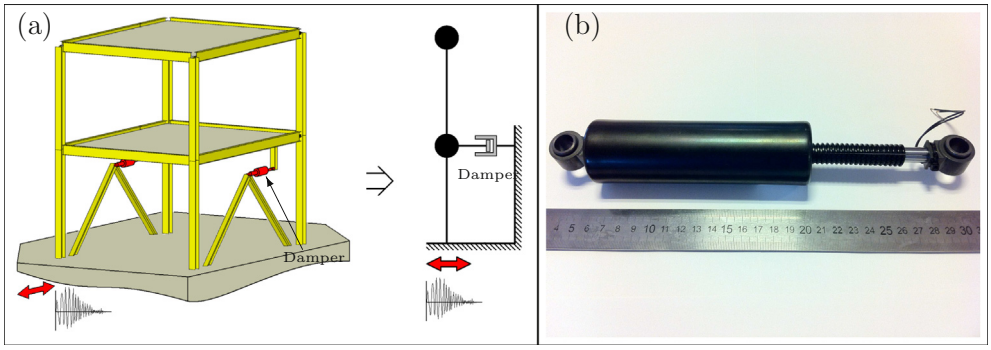

Fig. 2. (a) Ideal 2-DoF system with added passive dampers. (b) Real damper used in the experimental tests.

represent the optimal arrangement for the studied system, nevertheless this configuration is sufficient to gain a better understanding of the advantages of including an amplification mechanism together with the nonlinear dampers into a structure. The building has been modelled as a linear two degree-of-freedom (DOF) system by using Eq. (1), where M, C and K represent the mass, damping and stiffness matrices; $\ddot{x}, \dot{x}$ and x are the acceleration, velocity and displacement of the structure relative to the ground; $\ddot{x}_g$ is the ground acceleration, $\Gamma = [1,1]^T$ and $\Lambda = [-1,0]^T$.

$$M\ddot{x} + C\dot{x} + Kx = -M\Gamma\ddot{x}_g + \Lambda F_D \tag{1}$$

The structure is considered to be made of steel, the damping is fixed to be 3% of critical and the natural frequencies to be 2.086 and 5.46 Hz; and:

$$M = \begin{bmatrix} 1 & 0 \\ 0 & 1 \end{bmatrix} \times 145.8 \text{ N } \frac{\text{s}^2}{\text{m}}; \quad C = \begin{bmatrix} 248.9 & -83 \\ -83 & 165.9 \end{bmatrix} \text{N } \frac{\text{s}}{\text{m}};$$

$$K = \begin{bmatrix} 2 & -1 \\ -1 & 1 \end{bmatrix} \times 65.5 \ \frac{\text{kN}}{\text{m}} \tag{2}$$

In this study MR dampers are used in their passive mode (with the voltage set to zero), as the NLDs. The reason for selecting MR dampers is that the nonlinear dynamic modelling and associated parameter fitting for this type of damper is well developed. Here we use a simplified version of the Dahl model [15, p.152] as shown in Eq. (3), where F_D is the damper force in Newtons; $\dot{x}_D$ is the relative velocity across the damper in cm/s; t is time in seconds, $w \in (-1,1)$ is a dimensionless parameter which models the hysteresis in the force-velocity plane and ρ is a coefficient that controls the rate of change of the hysteric variable w. Note that both k_x and k_w are voltage-dependent parameters [16].

$$\begin{aligned} F_D(t) &= k_x(v)\dot{x}_D(t) + k_w(v)w(t) \\ \dot{w}(t) &= \rho(\dot{x}_D(t) - |\dot{x}_D(t)|w(t)) \end{aligned} \tag{3}$$

This model has proven to be accurate for describing the nonlinear behaviour of real dampers and captures the damper's response in the force-velocity plane while allowing a reduced number of parameters if compared against traditional hysteretic models like Bouc–Wen (Further details in [17]). A comprehensive work demonstrating the identification procedure can be found in [18].

Representing a generic amplification mechanism by means of an *amplification factor* (*AF*), enables us to write the velocity across the damper in terms of the relative velocity of the first floor of the structure, giving

$$\dot{x}_D = AF \times \dot{x}_1 \tag{4}$$

Hence the modified equations of the damper and amplifier combined are given by

$$\begin{aligned} F_D(t) &= AFk_x(v)\dot{x}_1(t) + k_w(v)w(t) \\ \dot{w}(t) &= \rho AF(\dot{x}_1(t) - |\dot{x}_1(t)|w(t)) \end{aligned} \tag{5}$$

For the physical damper discussed in Section 3, with a constant voltage of 0 V, the following set of parameters has been identified: $k_x(0) = 9.78$ N s cm^{-1}, $k_w(0) = 60.11$ N, $\rho = 47.95$ cm^{-1}. It is worth noting that the amplification factor only directly modifies the velocity-dependant terms in Eq. (5). This does not alter the magnitude of the term k_w but only the speed at which $w(t)$ changes from -1 to 1. To simulate the dynamic response of the structure, a numerical model has been developed in Mathworks Simulink. A range of numerical simulations have been performed to capture the changes in the structural behaviour. The parameter *AF* has been varied from 1 to 4 while different harmonic ground motion excitations have been applied to the system covering frequencies from 1.5 Hz and up to 5.5 Hz. Fig. 3a shows the numerical results for the steady-state energy dissipated per cycle for a single NLD. Similarly, Fig. 3b presents the numerical results for the maximum displacement (drift) reached at the level of the first floor. Note that the closest edge of both surfaces correspond to the case of no amplification ($AF = 1$).

The numerical results indicate that the larger the amplification factor, the larger the amount of energy dissipated by the damper and the lower the maximum storey drift reached. As expected, by amplifying the structural velocity across the dampers, a better structural performance is achieved as passive dampers move more readily into the slipping phase, generating larger forces and dissipating much more energy.

Nonetheless, the benefits of amplifying the velocity are only significant for a certain range of frequencies. Particularly, we observed that real advantages in terms of energy are achieved in between the first natural frequency and the anti-resonance frequency of the base structure (about 4.7 Hz). If reducing the floor displacement is the primary target when including the amplification mechanism, it must be optimised for a frequency slightly higher than the natural frequency of the original structure (around 2.4 Hz in the example). On the other hand, if increasing the energy dissipated is the main objective, then the frequency of interest in the example should be around 3.2 Hz. The simulations shown here are for a sinusoidal ground motion of 5 mm amplitude. Qualitatively very similar results were found for excitation amplitudes of 2.5 and 10 mm.

In order to compare this result with physical experiments, we tested a system equipped with real NLD. Fig. 2b shows the magnetorheological (MR) damper that was used in the experimental tests, a model RD-8040-1 produced by the Lord Corporation (see http://www.lord.com). It is characterised by a stroke of 55 mm and damping forces up to 2447 N (peak-to-peak) at 1 A. Note that we do not apply any voltage to the damper coils such that the damper can be considered as a purely passive NLD. In the next section, we introduce the experimental technique that was used and in Section 4 the experimental results are presented.

Two more examples are considered here. The aim is to show that the practical limit value of the *AF* beyond which the amplification mechanism loses effectiveness, is influenced by the

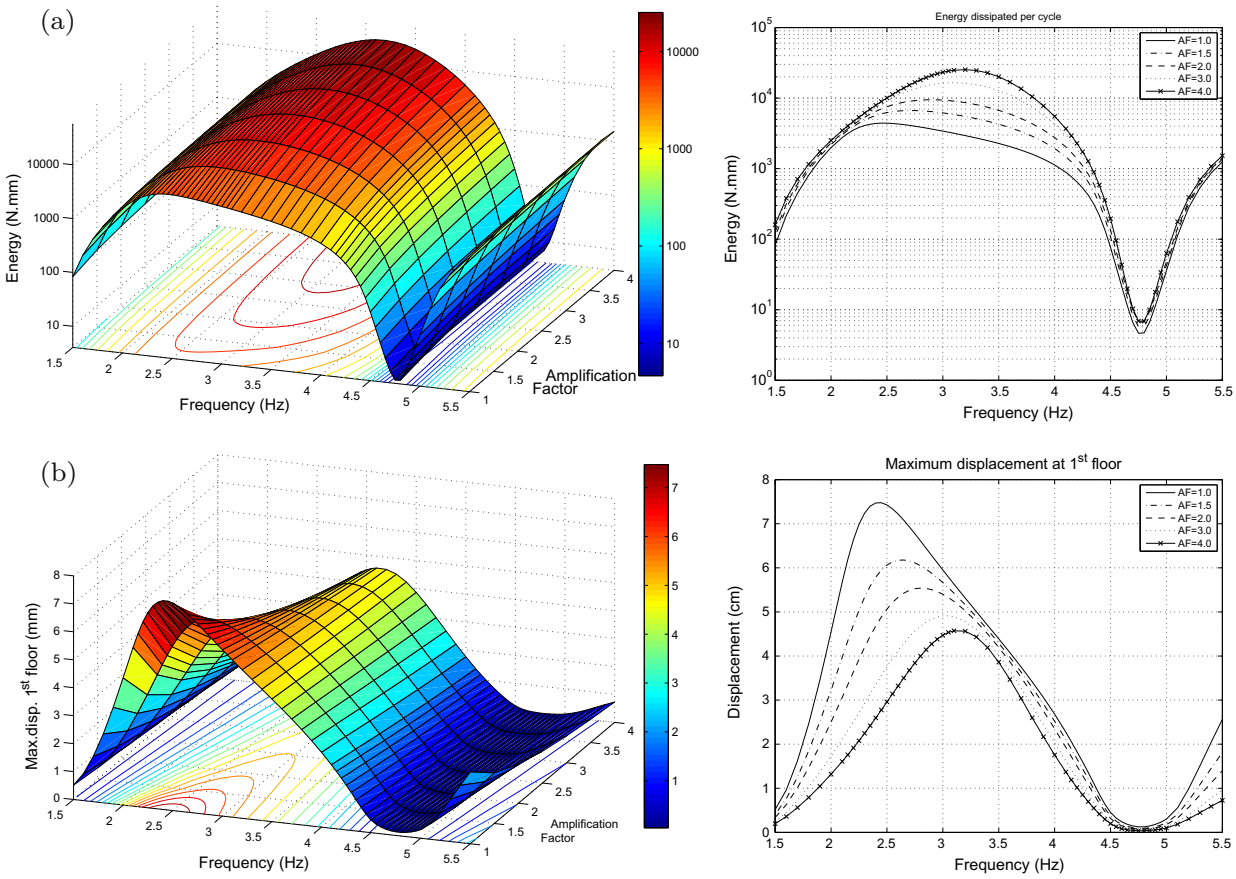

Fig. 3. Numerical simulations. (a) Energy dissipated per cycle in a single damper. (b) Maximum structural displacement at the first floor. The right hand side panels correspond to slices of the 3D surfaces for different levels of *AF*.

relative magnitude of the damping force with respect to the structural responses. In other words, it depends on the criteria used to size the dampers. Keeping the same damper size and similar additional damping ratio as a point of reference, the second example corresponds to the structural system presented in (2) with the masses increased by 50%. Fig. 4(a) presents numerical results of the energy dissipated per cycle in the steady-state in a single NLD (upper panel) along with the maximum drift reached at the first floor (lower panel). The third example corresponds to a 4-DOF system with same masses and stiffnesses as in (2) and nonlinear dampers located at the first and second floors. The numerical results are presented in Fig. 4(b). These results show again that there exists a practical limit for the amplification factor, beyond which the benefits of including the amplification mechanism are diminished. Larger values of the *AF* could be in fact detrimental as shown in the lower panel of Fig. 4(b), where the maximum displacement starts to rise as the *AF* exceeds the value of approximately 2.

3. Real-time dynamic substructuring testing

Real-time dynamic substructuring (RTDS) is an efficient and cost-effective testing technique able to assess the rate-dependent behaviour of systems. RTDS provides the ability to physically test mechanical components that are difficult to model numerically within a structure (due to, for example, their nonlinear behaviour) [19,20]. These components can be tested at real scale and in real-time to fully capture any rate dependency [21]. They are extracted from the original system to form the "physical substructure", while the remaining part of the system is simulated numerically (the "numerical substructure"). In RTDS forces and displacements must be matched at the interface between the two substructures, therefore dynamic transfer and measurement systems are included (see Fig. 5). The challenging issue is to minimise interface errors and therefore ensure that the physical and the numerical substructures together behave in the same way as the whole system [22,23].

In the experiments reported in this paper, the numerical substructure is the 2-DOF system described above (with no added damper), the physical substructure consists of the MR damper acting in passive mode and the transfer system is a electro-mechanical actuator. To satisfy compatibility and equilibrium at the interface, the interface displacement is calculated by the numerical substructure and posed to the physical substructure. The force required to impose this displacement is then passed back to the numerical substructure.

3.1. Delay, stability and accuracy

The success of a RTDS simulation is dependent on the performance of the actuator and its associated controller, whose dynamics introduce both timing and amplitude errors into the signal affecting the accuracy of the results [24]. Several authors have shown that these errors may be propagated throughout the simulation and may cause the test to become unstable [25,26]. Time delay compensation schemes, which make corrections on the actuator command signal, have commonly been used to overcome this issue [27]. The most-widely used procedure in RTDS simulation is the polynomial approximation method introduced by Horiuchi et al. [28–30]. Results of comparable quality using different compensation procedures can also be found in [31–33]. Due to

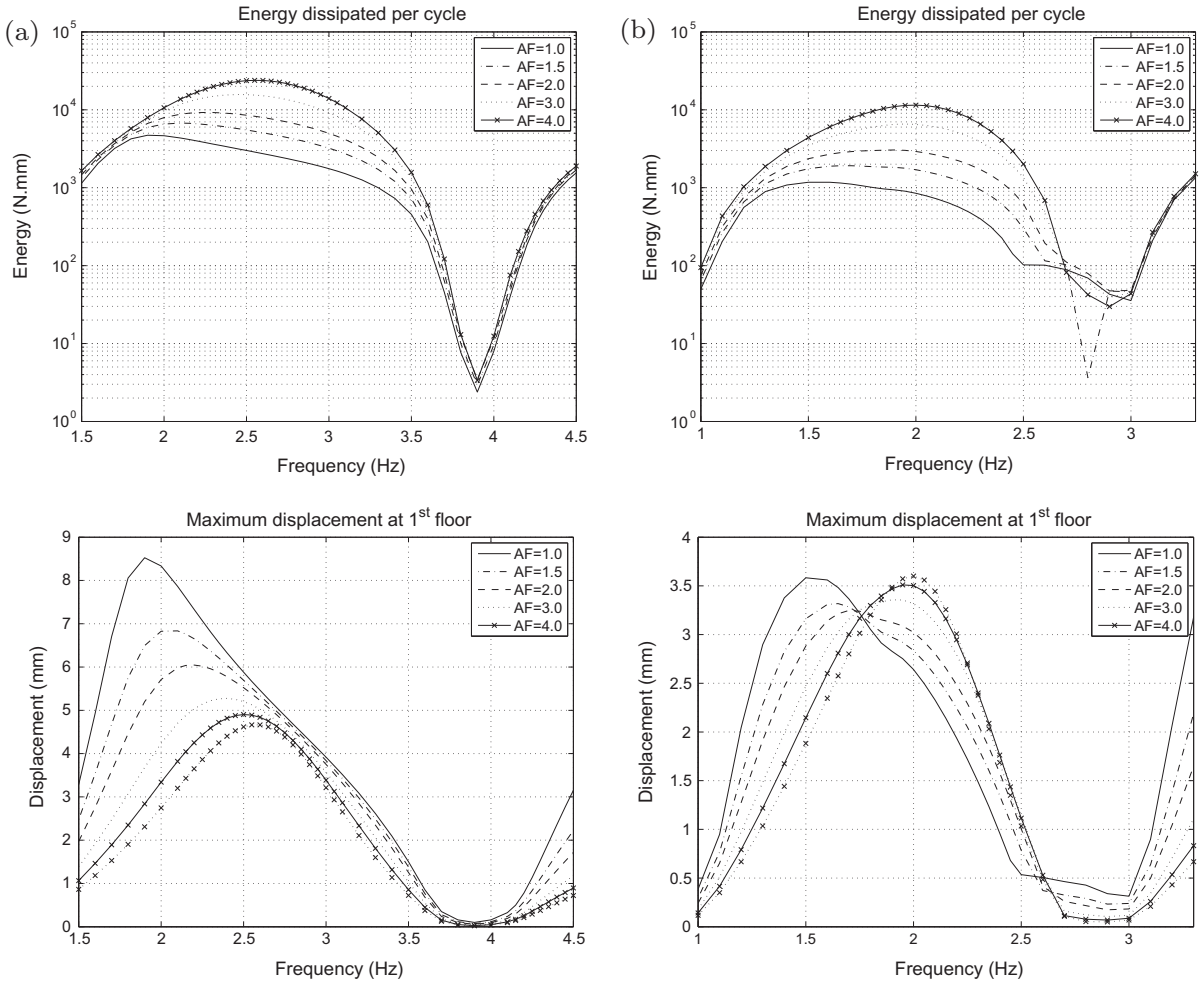

Fig. 4. Energy dissipated per cycle in a single damper in the first floor and the maximum structural displacement at the first floor: (a) if mass in Eq. (2) is increased by 50%; (b) if a 4-DOF systems is considered.

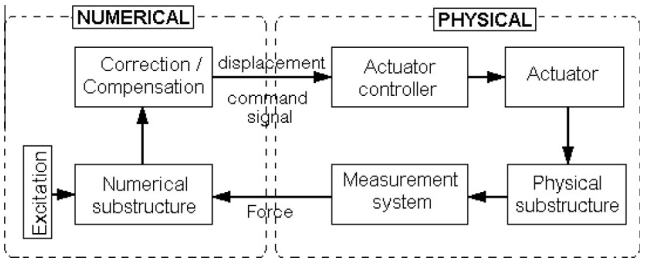

Fig. 5. Block diagram of a substructured system.

its simplicity and efficiency, a polynomial extrapolation scheme has been used in these experiments. Over the frequency range of interest, the actuator delay was found to be approximately constant at about 18 ms. We found that a first-order polynomial with four data points (with a spacing of 1 ms) can be used to successfully forward predict the command displacement.

Full numerical simulations have been completed to assess the effects of including both the damper nonlinearity and the delay compensation in the RTDS loop. In Fig. 6 the curves labelled "*No delay*" (solid line) correspond to the ideal RTDS outputs when neither delay nor compensation are considered; similarly, the curves labelled as "*Delayed*" (dashed line) correspond to the outputs when the actuator dynamics are modelled as a constant delay and a first-order polynomial is used to predict the actuator command signal. Fig. 6a shows the displacement time history at the first floor along with the damper force from formula (3); this simulation considers an actuator delay of 18 ms, $AF = 1$ and full delay compensation. The inclusion of both time lag and full delay compensation does not seem to alter the results significantly. However, when considering higher values of *AF* oscillations, which increase exponentially in amplitude, are observed in the simulation (See Fig. 6b where $AF = 3.25$).

We found that this phenomenon is due to the difficulty for a continuous-signal based predictor to cope with the near-piecewise response of the NLD. We note that the use of a higher-order polynomial does not provide any benefit as this just forces the system to undergo larger oscillations. By reducing the forward prediction, the tests can be stabilised for higher values of *AF* but with slightly reduced levels of accuracy. Fig. 6c shows a simulation where the prediction scheme compensates for 50% of the actuator delay. Note that the undesired oscillations decrease at shorter prediction times but they are always present to some extent.

Owing to the trade-off between stability, prediction and *AF*, the degree of forward prediction has individually selected for each experimental test presented in the next section. As *AF* increases, the forward prediction is reduced in such a way that the system was kept as close to the stability boundary as possible to maximise accuracy.

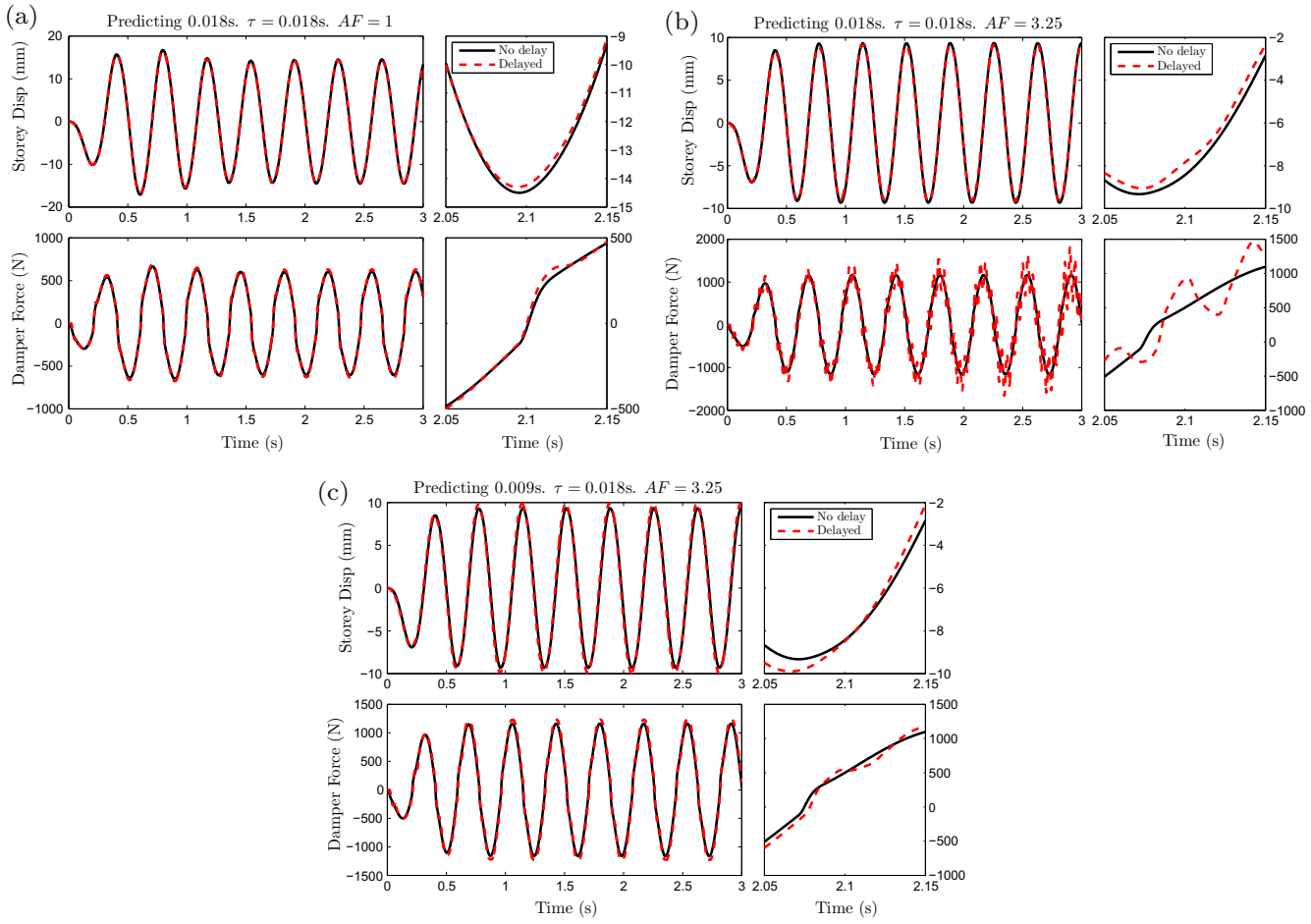

Fig. 6. Oscillations arise when errors in predicting piecewise signals are amplified by the *AF*.

4. Experimental results

The experimental rig shown in Fig. 7 has carefully been set up to emulate the structural system described in Section 2. A Dspace DS1104 board was used to run the numerical substructure and forward prediction written in Simulink.

The aim of these experiments was to physically test a system equipped with real NLDs and evaluate the effects of considering a motion amplification factor. Just as for the numerical simulations, the structural model has been evaluated under ground excitation using harmonic motion and the mechanical amplifier has been modelled as a constant gain.

4.1. Harmonic excitation

Several tests were conducted to capture the changes in the system behaviour when the velocity transferred to the damper is amplified. Fig. 8 shows the damper response for 4 different levels of amplification when the structure is excited at 3.0 Hz and 5 mm. As can been seen, the nature of the damper response is highly non-linear. From the figure it is also clear how much energy is dissipated by the damper as *AF* increases. For the experiments, we have considered ground motion excitations at frequencies from 1.5 to 5.5 Hz in steps of 0.5 Hz. Higher frequencies were not considered here since they fall outside the range of the test equipment. The system has been evaluated for the cases when the velocity transferred to the damper was amplified by factors of 1.0, 1.5, 2.0, 3.0 and 4.0. This range of parameters was also determined in accordance with the physical limitation of the damper (after amplification the maximum damper displacement is 23 mm).

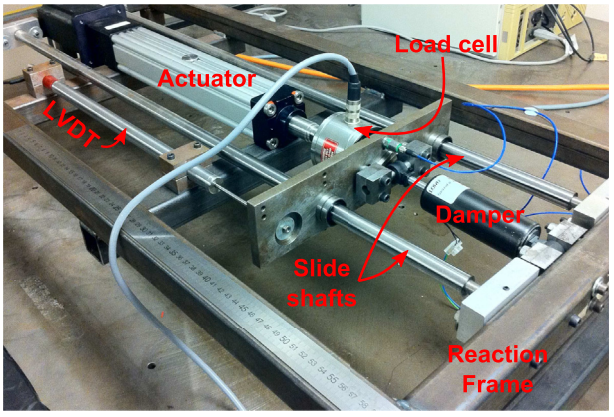

Fig. 7. Experimental rig used for running the RTDS simulations.

Figs. 9b and 10b summarise the experimental steady-state responses. In these plots, the black dots correspond to direct experimental measurements while the surfaces were constructed within the range of the discrete set of known data points by using the cubic spatial interpolation method. The numerical results have been included again to facilitate a direct comparison (panel a) in both figures). The figures demonstrate very good agreement between the numerical estimations and the experimental results.

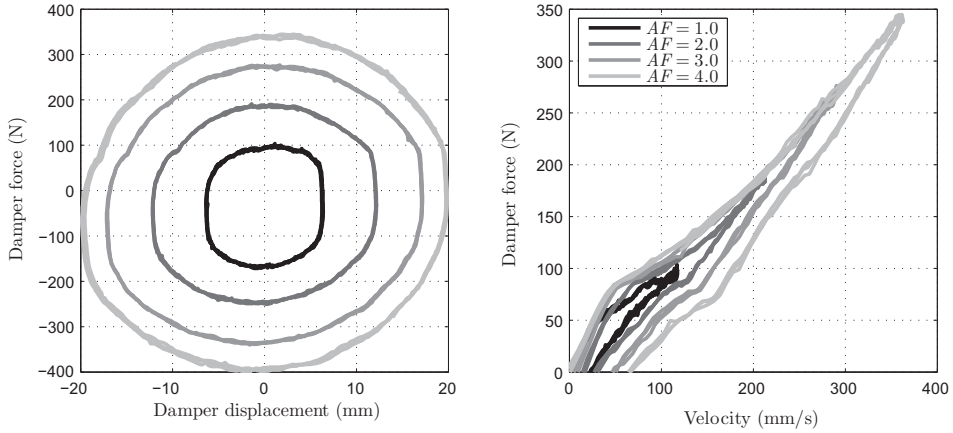

Fig. 8. Damper response at different values of the amplification factor *AF* when structure is excited at 3.0 Hz.

The experimental tests confirm that the amplification of the structural displacements and velocities transferred to the supplemental dampers can improve the structural performance in a range of frequencies that goes from just beyond the natural frequency to the anti-resonance frequency of the unmodified structure. From both numerical and experimental results it has been observed that no significant benefits are achieved for amplification factors greater than 3 as only limited further reduction in structural response is achieved beyond this point. This suggests that well-behaved mechanism-damping systems are required to offer amplification up to approximately 3 times, beyond this value the mechanism would be over-specified for this damper setup.

4.2. Seismic excitation

We now consider the case of the structure subjected to seismic base excitation. The earthquake considered is compatible with the elastic response spectrum provided by Eurocode 8 for very dense sand, gravel, or very stiff clay (soil type B) and for high and moderate seismicity regions (Seismic Zone 1), but has been scaled in amplitude as shown in Fig. 11a in accordance with the physical constrains of the damper and experimental rig. We note that the earthquake was chosen so that the maximum frequency content of the ground motion occurs around the first natural frequency of the structure. Fig. 11b presents a typical response when carrying out a substructuring simulation of the whole system with the selected seismic load. The plots correspond to the case of an amplification factor of 2.5. The total energy dissipated during the strongest part of the earthquake (5 to 20 s) is 78.99 Nm.

The experimental results considering seismic base excitation are summarised in Fig. 12, where both the total energy dissipated by the dampers and the maximum structural displacement at the first floor have been plotted against the amplification factor. As the amplification factor increases the system exhibits a significant reduction of the structural displacements and a corresponding increase in the amount of energy dissipated during the earthquake. As with the harmonic excitation results, the effects of increasing the amplification become less at higher amplification factors. Note that considering softer soil conditions, or equivalently earthquakes with frequency contents outside the considered frequency range, will not have significant impact in the structural response and therefore the study regarding the effects of the *AF* will be less meaningful.

4.3. Effects of the mechanism flexibility

The flexibility of the amplification mechanism could significantly reduce its own efficiency and therefore diminish the damping capability of the mechanism-damping arrangement. Due to the mechanism compliance, the amplified displacement that is actually transferred from the amplification device to the damper is reduced. Compliance also introduces a phase offset (with reference to the structural forcing displacement) in the damper response. These issues have been studied when searching for more accurate design procedures of brace-damper systems [34].

To assess the impact of compliance on the overall system performance, we introduce the mechanism stiffness effect into the model by way of a linear spring. This flexible element was located

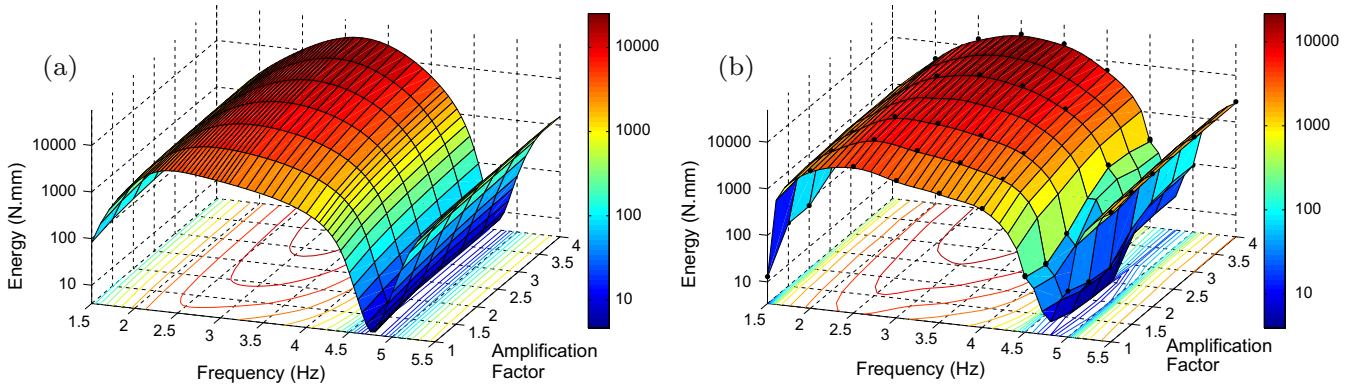

Fig. 9. Energy dissipated per cycle in a single damper. (a) Numerical simulations. (b) Experimental results.

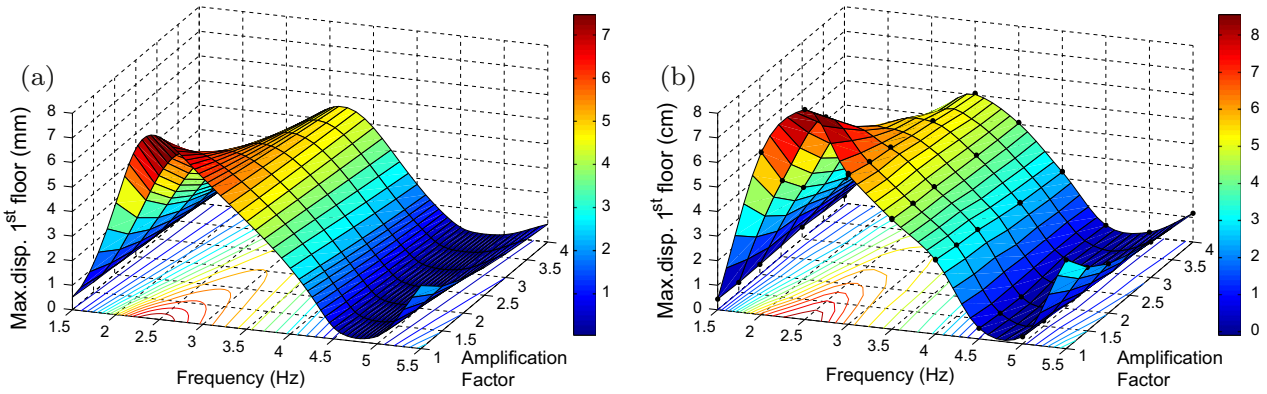

Fig. 10. Maximum structural displacement at the first floor. (a) Numerical simulations. (b) Experimental results.

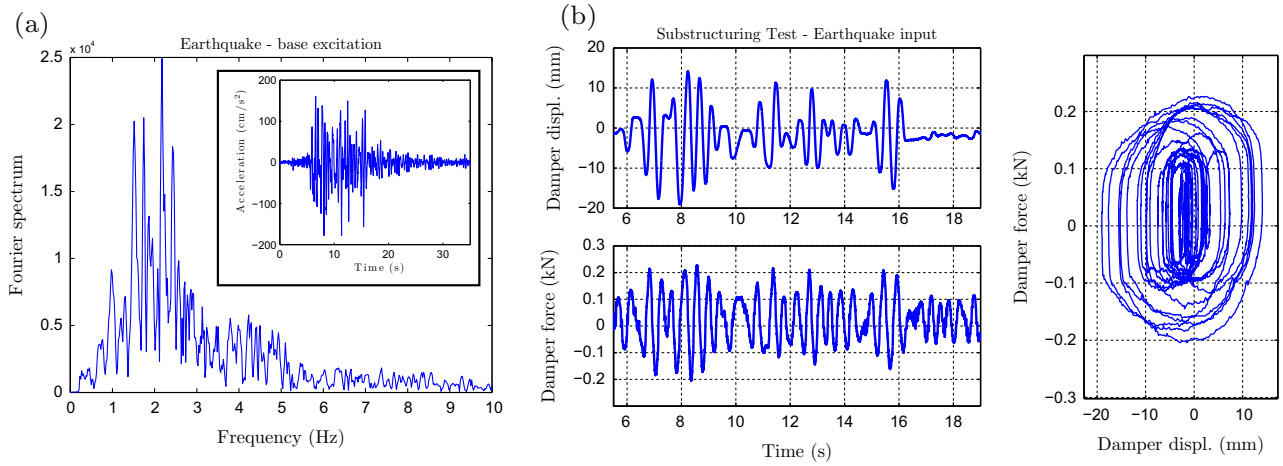

Fig. 11. (a) Earthquake ground motion used in the tests. (b) Experimental response of the system for $AF = 2.5$.

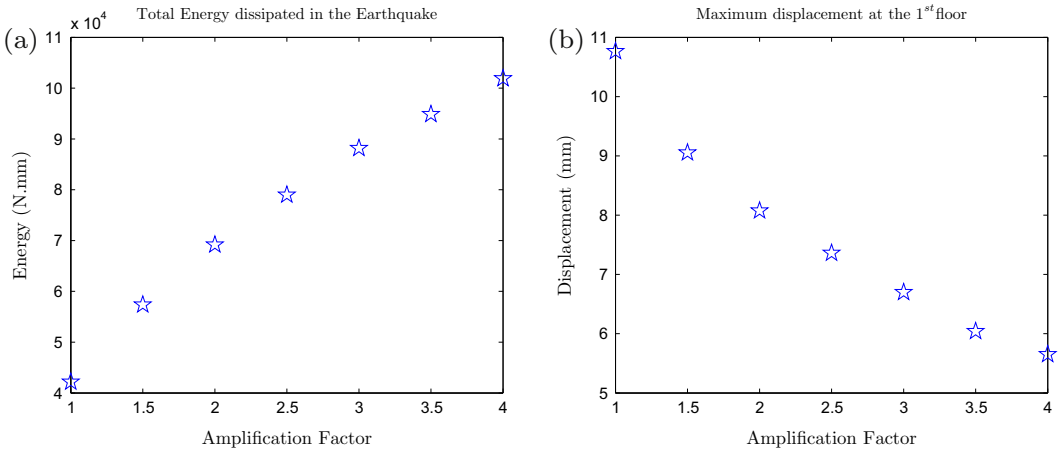

Fig. 12. Experimental results considering seismic base excitation. (a) Total energy dissipated by a single damper. (b) Maximum structural displacement at the first floor.

in series between the generic amplification mechanism and the damper. Simulations in which the ratio of mechanism stiffness (k_m) to structural stiffness (k_s) was varied have been conducted. Fig. 13a shows how the energy dissipated per cycle is affected as the ratio k_s/k_m increases. The surfaces are coloured in grayscale with the darkest colour corresponding to the more compliant mechanism configuration.

Fig. 13b shows the maximum displacement at the first floor for the structure when considering a mechanism with $AF = 1$ and varying k_s/k_m at the frequency of 2.4 Hz that corresponds to the peak displacement for the system without mechanism ($AF = 1$, $k_m \to \infty$). The dashed line indicates the level of displacement reached when no amplification mechanism is considered. The plot shows the degradation in the structural response as the

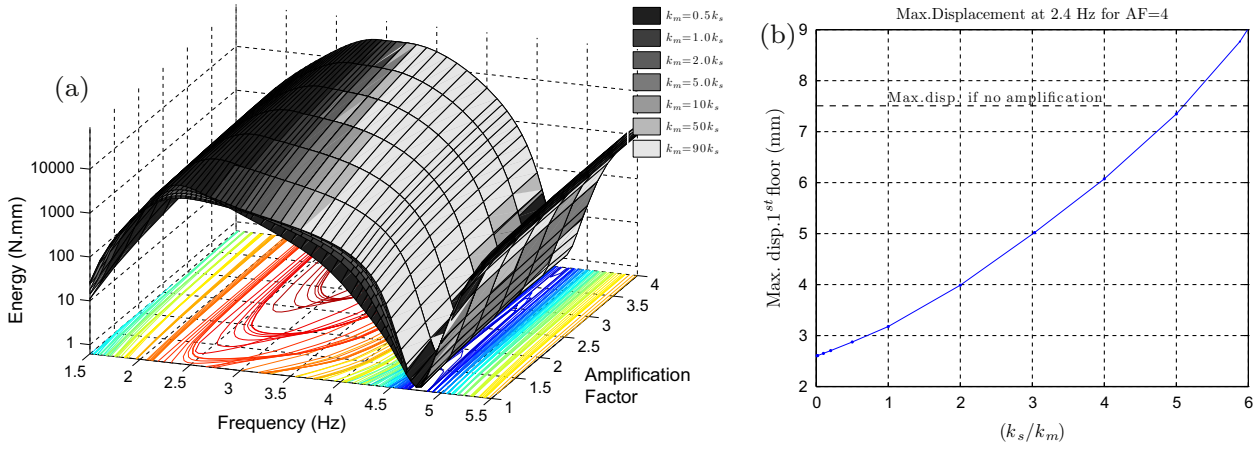

Fig. 13. Effects of the mechanism stiffness (k_m) on the system performance: (a) impact on the energy dissipated by the damper; (b) impact on the maximum structural displacement at the first floor.

mechanism flexibility increases. For stiffnesses k_m lower than 20% of the floor stiffness, the beneficial effect of the mechanical amplification is no longer seen – in fact the presence of the mechanism is deleterious in this case.

5. Conclusions

In this paper we investigated the advantages of amplifying the structural velocity transmitted to non-linear dampers (NLD) fitted within a structure. We tested a small NLD attached to an amplification mechanism and presented results for a series of numerical simulations. These findings were verified experimentally using real-time dynamic substructuring with a real damper. We found that the structural performance can be improved if an amplification mechanism-damping system is added to increase the sensitivity of the NLD as they spend more time in the slipping phase. Nonetheless, such benefits are only significant for a range of frequencies that goes from just beyond the first natural frequency to the anti-resonance frequency of the unmodified structure and for amplification factors between 1 and 3 in the cases studied. Beyond this range the amplification mechanism would be overspecified for the tested setup. We note that this practical limit of the amplification factor is influenced not only by the nonlinear characteristics of the damper, but also by the relative magnitude of the damping force with respect to the structural responses, i.e. it depends on the criteria used to size the dampers.

Excitation frequencies higher than 5.5 Hz could not be tested experimentally since they fall outside the range of the test equipment. Yet numerical simulations indicate no significant improvement above that range for any value of *AF*. This can be explained by the fact that the overall system response (including the mechanism) is moved away from the resonance region.

The impact of the mechanism compliance on the vibration suppressions was also studied. We showed the degradation in the structural response as the mechanism flexibility increases. We found that for mechanisms with an effective stiffnesses lower than 20% of the structural stiffness, the beneficial effect of the mechanical amplification is no longer seen. This demonstrates the need to carefully design the mechanism to achieve the wanted performance in terms of energy dissipation and storey drift.

Acknowledgement

J.M. Londoño was funded by the Royal Society and the Royal Academy of Engineering of the United Kingdom through a Newton International Fellowship (http://www.newtonfellowships.org/). S.A. Neild is funded by a EPSRC fellowship, EP/K005375/1. This financial support is gratefully acknowledged.

References

[1] Spencer BF, Nagarajaiah S. State of the art in structural control. ASCE J Struct Eng 2003;129(7):845–56.
[2] Wagg DJ, Neild SA. A review of non-linear structural control techniques. Proc Inst Mech Eng C J Mech Eng Sci 2011;225(4):759–70. http://dx.doi.org/10.1177/2041298310392855.
[3] Ribakov Y, Gluck J, Gluck N. Practical design of mdof structures with supplemental viscous dampers using mechanical levers. In: Proc of the 8th ASCE specialty conference on probabilistic mechanics and structural reliability; 2000.
[4] Ribakov Y, Reinhorn AM. Design of amplified structural damping using optimal considerations. J Struct Eng 2003;129(10):1422–7. http://dx.doi.org/10.1061/(ASCE)0733-9445(2003)129:10(1422).
[5] Gluck J, Ribakov Y. Active viscous damping system with amplifying braces for control of MDOF structures. Earthquake Eng Struct Dynam 2002;31(9):1735–51. http://dx.doi.org/10.1002/eqe.202.
[6] Zasso A, Aly A, Resta F. MR dampers with lever mechanism for response reduction in high-rise buildings under wind loads. In: Proc. 5th European & African conference on wind engineering, Florence, Italy; 2009.
[7] Constantinou MC, Tsopelas P, Hammel W. Testing and modeling of an improved damper configuration for stiff structural systems, Tech. rep., <http://www.taylordevices.com/Tech-Paper-archives/literature-pdf/50-Testing-Modeling.pdf>, Center for Industrial Effectiveness and Taylor Devices, Inc.; 1997.
[8] Constantinou MC, Tsopelas P, Hammel W, Sigaher AN. Toggle-brace-damper seismic energy dissipation systems. J Struct Eng ASCE 2001;127(2):105–12.
[9] Lee SH, Min KW, Chung L, Lee SK, Lee MK, Hwang J-S, Choi S-B, Lee H-G. Bracing systems for installation of MR dampers in a building structure. J Intell Mater Syst Struct 2007;18(11):1111–20. http://dx.doi.org/10.1177/1045389X06072371.
[10] Şigaher AN, Constantinou MC. Scissor-jack-damper energy dissipation system. Earthquake Spectra 2003;19(1):133–58. http://dx.doi.org/10.1193/1.1540999.
[11] Berton S, Bolander JE. Amplification system for supplemental damping devices in seismic applications. J Struct Eng ASCE 2005;131(6):979–83. http://dx.doi.org/10.1061/(ASCE)0733-9445(2005)131:6(979).
[12] Hwang JS, Kim J, Kim YM. Rotational inertia dampers with toggle bracing for vibration control of a building structure. Eng Struct 2007;29(6):1201–8. http://dx.doi.org/10.1016/j.engstruct.2006.08.005.
[13] Hwang JS. Seismic design of structures with viscous dampers. In: International training programs for seismic design of building structures. National Center of Research on Earthquake Engineering of Taiwan; 2000.
[14] Spizzuoco M, Londoño JM, Serino G. An experimental campaign on a passively controlled building structure. In: Proceedings of the fourth european conference of structural control. vol. 2, St. Petersburg, Russia, isbn: 978-5-904045-10-4; 2008. p. 950–9.
[15] Ikhouane F, Rodellar J. Systems with hysteresis: analysis. In: Identification and control using the Bouc–Wen model. John Wiley & Sons, Inc; 2007.
[16] Aguirre N, Ikhouane F, Rodellar J. Proportional-plus-integral semiactive control using magnetorheological dampers. J Sound Vib 2011;330(10):2185–200. http://dx.doi.org/10.1016/j.jsv.2010.11.027.
[17] Ikhouane F, Dyke SJ. Modeling and identification of a shear mode magnetorheological damper. Smart Mater Struct 2007;16(3):605–16. http://dx.doi.org/10.1088/0964-1726/16/3/007.
[18] Ikhouane F, Rodellar J. On the hysteretic Bouc–Wen model. Part II: Robust parametric identification. Nonlinear Dynam 2005;42(1):79–95. http://dx.doi.org/10.1007/s11071-005-0070-x.

[19] Bursi OS, Wagg DJ, editors. Modern testing techniques for structural systems dynamics and control. CISM international centre for mechanical sciences, vol. 502. Springer; 2008.
[20] Shao X, Reinhorn AM. Unified formulation for real time dynamic hybrid testing. In: Yuan Y, Cui J, Mang H, editors. Computational structural engineering. Netherlands: Springer; 2009. p. 201–8. http://dx.doi.org/10.1007/978-90-481-2822-8_23.
[21] Gawthrop PJ, Wallace MI, Neild SA, Wagg DJ. Robust real-time substructuring techniques for under-damped systems. Struct Control Health Monit, vol. 14. john Wiley & Sons, Ltd; 2007. p. 591–608. http://dx.doi.org/10.1002/stc.174.
[22] Neild SA, Stoten DP, Drury D, Wagg DJ. Control issues relating to real-time substructuring experiments using a shaking table. Earthquake Eng Struct Dynam, vol. 34. john Wiley & Sons, Ltd.; 2005. p. 1171–92. http://dx.doi.org/10.1002/eqe.473.
[23] Shao X, Reinhorn A, Sivaselvan M. Real-time hybrid simulation using shake tables and dynamic actuators. J Struct Eng 2011;137(7):748–60. http://dx.doi.org/10.1061/(ASCE)ST.1943-541X.0000314.
[24] Wallace MI, Sieber J, Neild SA, Wagg DJ, Krauskopf B. Stability analysis of real-time dynamic substructuring using delay differential equation models. Earthquake Eng Struct Dynam, vol. 34. john Wiley & Sons, Ltd; 2005. p. 1817–32. http://dx.doi.org/10.1002/eqe.513.
[25] Wagg DJ, Stoten DP. Substructuring of dynamical systems via the adaptive minimal control synthesis algorithm. Earthquake Eng Struct Dynam 2001;30:865–77. http://dx.doi.org/10.1002/eqe.44.
[26] Londoño JM, Serino G, Wagg DJ, Neild SA, Crewe AJ. On the assessment of passive devices for structural control via real-time dynamic substructuring. Struct Control Health Monit 2012;19(8):701–722 http://dx.doi.org/10.1002/stc.464.
[27] Bursi O, He L, Lamarche C, Bonelli A. Linearly implicit time integration methods for real-time dynamic substructure testing. J Eng Mech 2010;136(11):1380–9. http://dx.doi.org/10.1061/(ASCE)EM.1943-7889.0000182.
[28] Horiuchi T, Inoue M, Konno T, Namita Y. Real-time hybrid experimental system with actuator delay compensation and its application to a piping system with energy absorber. Earthquake Eng Struct Dynam, vol. 28 (10). John Wiley & Sons, Ltd; 1999. p. 1121–41. http://dx.doi.org/10.1002/(SICI)1096-9845(199910)28:10<1121::AID-EQE858>3.0.CO;2-O.
[29] Nakashima M, Masaoka N. Real-time on-line test for MDOF systems. Earthquake Eng Struct Dynam, vol. 28 (4). John Wiley & Sons, Ltd; 1999. p. 393–420. http://dx.doi.org/10.1002/(SICI)1096-9845(199904)28:4<393::AID-EQE823>3.0.CO;2-C.
[30] Darby AP, Williams MS, Blakeborough A. Stability and delay compensation for real-time substructure testing. J Eng Mech 2002;128(12):1276–84. http://dx.doi.org/10.1061/(ASCE)0733-9399(2002)128:12(1276).
[31] Ahmadizadeh M, Mosqueda G, Reinhorn AM. Compensation of actuator delay and dynamics for real-time hybrid structural simulation. Earthquake Eng Struct Dynam, vol. 37. john Wiley & Sons, Ltd; 2008. p. 21–42.
[32] Wallace MI, Wagg DJ, Neild SA. An adaptive polynomial based forward prediction algorithm for multi-actuator real-time dynamic substructuring. Proc Roy Soc A Math Phys Eng Sci 2005;461(2064):3807–26. http://dx.doi.org/10.1098/rspa.2005.1532.
[33] Bonnet PA, Williams MS, Blakeborough A. Compensation of actuator dynamics in real-time hybrid tests. Proc Inst Mech Eng I J Syst Control Eng 2007;221(2):251–64. http://dx.doi.org/10.1243/09596518JSCE301.
[34] Londoño JM, Neild SA, Wagg DJ. A noniterative design procedure for supplemental brace-damper systems in single-degree-of-freedom systems. Earthquake Eng Struct Dynam 2013;42(15):2361–7. http://dx.doi.org/10.1002/eqe.2339.